Improvement of mechanical properties and surface finish of 3d-printed polylactic acid parts by constrained remelting

Hong-Cheol Kim[1], Da-Yeong Kim[1], Ji-Eun Lee[1,2], Keun Park[1*]

[1]*Department of Mechanical System Design Engineering, Seoul National University of Science and Technology, 232 Gongneung-ro, Nowon-gu, Seoul, 01811, Republic of Korea*
[2]*Micro/Nano Scale Manufacturing R&D Group, Korea Institute of Industrial Technology, 143 Hanggaul-ro, Sangnok-gu, Ansan,15588, Republic of Korea*

[*]Corresponding author: Tel: (+82) 2 970 6358; E-mail: kpark@seoultech.ac.kr

Received: 15 February 2017, Revised: 04 April 2017 and Accepted: 09 April 2017

DOI: 10.5185/amlett.2017.1686
www.vbripress.com/aml

Abstract

According to recent advancements in additive manufacturing (AM) technology, also known as 3d printing, the role of AM has changed from the conventional rapid prototyping (RP) to direct fabrication of functional parts. The AM technology based on layer-by-layer manufacturing has a limitation in its poor surface finish and mechanical strength, especially along the thickness direction. This study proposes a new post-processing method for thermoplastic AM products with the goal of improving surface finish and mechanical strength. The proposed method, called *constrained remelting*, uses a metal mould with a negative shape that surrounds the printed polymer part. This mould is heated near the melting temperature of the polymer material so that the printed sample is melted and reshaped inside the mould. To evaluate changes in surface finish and mechanical strength, tensile specimens were printed and tested with various build directions; the tensile test revealed that the *Z*-directionally printed specimen had much lower mechanical strength than the specimens built along *X*- or *Y*- directions. Remelting experiments were then performed for the *Z*-directionally printed specimen under various remelting conditions (remelting temperature and initial thickness), and the resulting changes in surface finish and tensile strength were investigated. Among these remelting conditions, the 160°C remelting temperature and 4.0 mm thickness condition provided the best result where surface finish and tensile strength were improved significantly so as to be comparable to those of injection-moulded products.

Keywords: 3d printing, additive manufacturing, surface finish, tensile strength, constrained remelting.

Introduction

Additive manufacturing (AM), also called 3d printing, is used to express layer-by-layer manufacturing in contrast to the traditional subtractive manufacturing [**1**]. In past years, the layer-by-layer manufacturing had been called rapid prototyping (RP) because its main goal was to make prototypes before the mass-production stage [**2**]. This RP technology was changed to AM technology, as the development of 3d printers with high quality and performance has driven their applications to direct fabrication of functional parts [**3**]. A 3d-printed part, however, has poor surface finish and mechanical strength along the thickness direction due to its intrinsic layer-by-layer manufacturing [**4**], which needs to be improved in order to be used as an end product.

Among various AM technologies, material extrusion type (commonly known as fused deposition modeling or FDM) 3d printers were most popularly used; many FDM type 3d printers were developed after the Reprap project [**5**], an open source project to develop FDM type personal printers. FDM type printers use thermoplastic polymer filaments as base material and have advantages in simple equipment setup and low material cost. However, they have a disadvantage in surface finish because their layer thicknesses are usually thicker than 0.1 mm due to the limit in the extrusion nozzles diameter [**6**]; this layer thickness is much larger than those of other printing methods such as photo-polymerization or power-bed fusion types.

To improve surface finish of 3d-printed parts using FDM type printers, various approaches have been studied: determination of optimal building direction [**7-9**], mechanical machining [**10-12**], abrasive flow finishing [**13**], and chemical treatments [**14-16**]. Although these approaches could improve surface finish of 3d-printed parts, they cannot enhance mechanical strength in the thickness direction (*Z*-direction), which is known to be much inferior to those in the in-plane directions (*X*- or *Y*-directions) [**17**].

In this study, we developed *constrained remelting*, a new post-processing method for improving surface finish as well as mechanical strength for 3d printed parts. In this process, a negative mould was prepared to surround a 3d-printed sample and was heated near the melting temperature of the printed material so that the printed sample was melted and reshaped inside the heated mould. To evaluate changes in the surface finish and mechanical strength, tensile test specimens were printed using an FDM-type 3d printer, and a remelting mould with a negative shape was prepared accordingly. Remelting experiments were then performed under various remelting conditions, and the resulting changes in surface finish and mechanical strength are discussed.

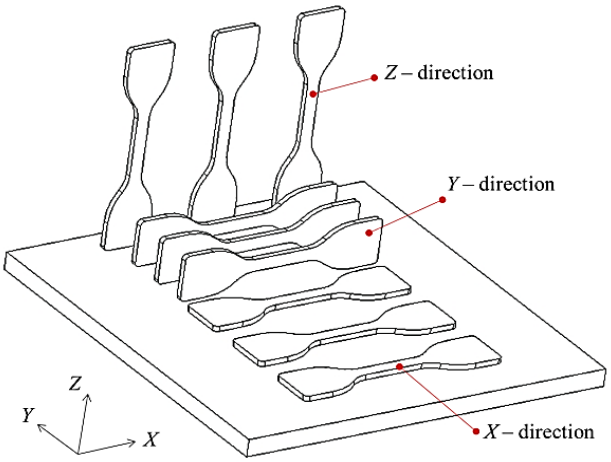

Fig. 1. Building direction of tensile specimens using 3d printing.

Experimental

Materials

For 3d printing, semi-transparent polylactic acid (PLA) filaments of 1.75 mm diameter (PLA-GP05NA, Canon Korea Business Solutions Inc., Korea) were used. AA6061 was used to fabricate the remelting mould, and its thermal properties are listed in **Table 2**, as supporting information. Al_2O_3-based ceramic boards with a thickness of 5.0 mm (Hanmi Refractories, Korea) were used as insulation plates, which had a thermal conductivity of 0.07 W/m-K.

3D printing

3D printing was performed using an FDM type 3D printer (MARV, Canon Korea Business Solutions Inc., Korea). ASTM D638 tensile test specimens (type IV, thickness: 3 mm) were designed and printed. To investigate the effect of building directions on the mechanical properties, the tensile specimens were printed along three directions: *X*, *Y*, and *Z* directions as illustrated in **Fig. 1**. The extrusion temperature was set to 200 °C. The feed rate and layer thickness were set to 40 mm/s and 0.2 mm, respectively.

Constrained remelting

To perform constrained remelting for 3d-printed specimens, a remelting mould was prepared as shown in **Fig. 2a**. A profiled mould insert with a thickness of 3.0 mm was manufactured with a negative shape of the tensile specimen and was inserted between the upper and lower moulds. A heating channel and three cooling channels were fabricated in each side, and a temperature sensor was inserted near the lower heating channel. Two cartridge heaters of 150 W were inserted in these heating channels, and cold water was circulated in the upper and lower cooling channels. This mould was then installed in a press machine, and the remelting experiments were performed after the mould was closed.

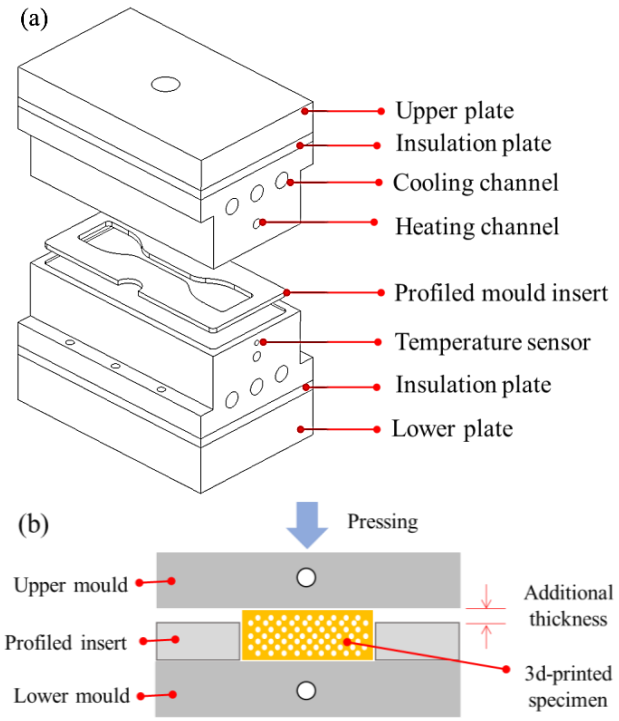

Fig. 2. (a) Configuration of constrained remelting apparatus for 3d-printed specimens, (b) Description of the additional thickness of a specimen.

The remelting procedure consisted of two stages, heating and cooling. In the heating stage, the upper and lower moulds were heated by two cartridge heaters. The mould temperature was controlled to remain below the melting temperature of the polymer material at 140, 150, and 160°C. In the cooling stage, the mould temperature was maintained at 35°C by circulating cold water. The heating and cooling times were set to 10 and 1 minute, respectively, in order to ensure sufficient remelting and cooling of the PLA specimens. To justify these conditions, numerical simulation results are provided in the *Supporting Information* part.

Fig. 2b shows the sectional configuration of the remelting region. It can be seen that the mould may be closed completely or not, according to initial thickness of the specimen; the mould cannot be closed completely when the specimen is thicker than the profiled mould insert, which is 3.0 mm thick. This additional thickness in the constrained remelting is given in order to compensate for the volume loss due to porosity of the 3d-printed specimens, by providing additional material.

Characterizations

To measure thermal properties of PLA, a differential scanning calorimetric (DSC) test was performed for the PLA sample. A DSC thermal analyzer (Q20, TA Instruments, USA) was used at a rate of 10 °C/min from 20 to 250 °C in a nitrogen atmosphere. Tensile tests were performed using a universal test machine (NA-2M, Nanotech, Korea), four samples for each building direction. The surface roughness of the printed samples was measured using a surface roughness tester (Rugosurf 90G, TESA Technology, Switzerland). A digital optical microscope (Mi-9000, Jason Electro-Tech, Korea) was used to observe sectional images of the printed parts.

Results and discussion

Basic properties of 3d printed samples

Fig. 3 plots the DSC curve for the 3d-printed PLA sample. The melting temperature and glass transition temperature were 167.2 and 62.9 °C, respectively. Based on this result, the remelting temperature was set to be between the glass transition and melting temperatures: 140, 150, and 160°C.

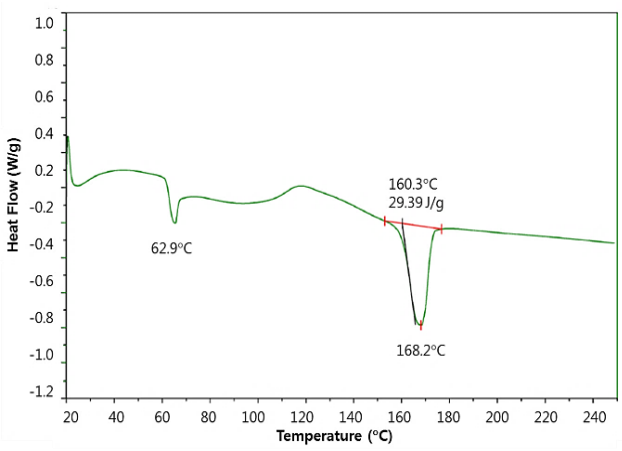

Fig. 3. DCS curve for the 3d-printed PLA sample.

Table 1. Mechanical properties according to the printing directions.

Building direction	*X*	*Y*	*Z*
Elastic modulus (GPa)	4.17	3.99	2.40
Tensile strength (MPa)	34.3	32.1	14.7
Elongation (%)	1.40	1.07	0.57

Table 1 compares mechanical properties of the 3d-printed specimens through the tensile test according to their building directions. The Z-directionally printed specimen has much lower mechanical properties than those of the *X*- or *Y*-directionally printed specimens. This degeneration in mechanical properties originated from the unique building characteristics of 3d printing; the specimen was laminated along its longitudinal direction. Therefore, the tensile failure occurred not by a tensile fracture but by delamination between laminated layers.

Effect of remelting conditions

Fig. 4a illustrates photographs of the remelted specimens under the three temperature conditions. It can be seen that the remelted specimen at 140 °C looks opaque, which is similar to the pure printed sample without remelting. On the other hand, specimens at 150 °C and 160 °C remelting changed to semi-transparent. These results indicate that the remelting under a temperature higher than 150°C resulted in re-joining of the laminated layers.

Fig. 4b shows cross-sectional photographs of the remelted specimens at 160°C, which shows a number of voids at various locations. These voids can be explained by a lack of material volume. That is, a number of porous spaces exist inside the printed part among the laminated filaments. Thus, the total volume decreased when these porous spaces were filled with molten polymer material, and then larger voids were generated.

To overcome such a void generation, the tensile specimens were fabricated with increased thicknesses: 3.5 and 4.0 mm. The specimens with increased thicknesses were then installed in the remelting apparatus as illustrated in **Fig. 2b**. The relevant results will be discussed in the next sections.

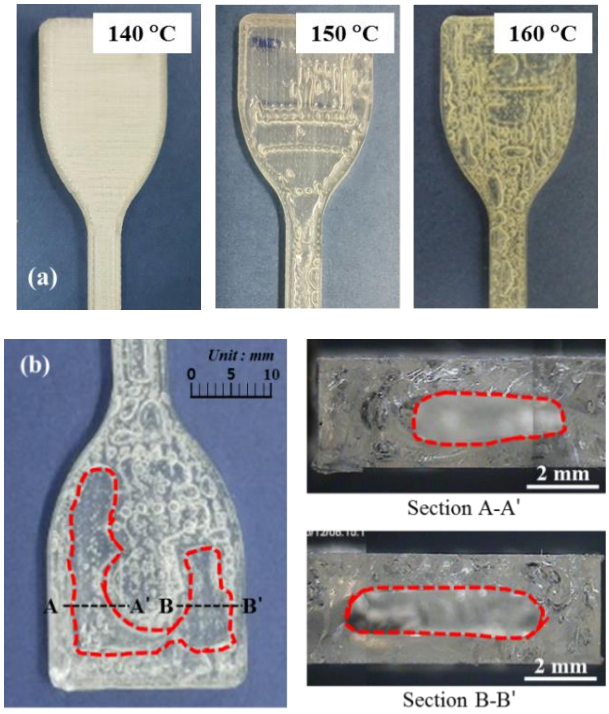

Fig. 4. (a) Outer appearance of 3d-printed specimens according to remelting temperature, (b) Sectional photographs of a remelted sample (remelting temperature: 160 °C).

Surface roughness

Fig. 5a plots the variation of surface roughness (R_a) according to the remelting temperature for the specimens with a 3.0 mm initial thickness. The surface roughness of the pure printed specimens was 13.06 μm. This roughness was slightly reduced to 13.01 μm when the remelting temperature was 140 °C, which means that the remelting was sufficient to reduce surface roughness. In the cases of 150 and 160 °C temperatures, on the other hand, the surface

roughness was reduced significantly to 0.52 and 0.47 μm, respectively.

The remelting temperature was then set to 160°C, and remelting experiments were performed for three specimens with various thicknesses: 3.0, 3.5, and 4.0 mm. **Fig. 5b** compares the variation in surface roughness according to the initial thickness. It can be seen that the surface roughness was significantly reduced below 1.0 μm in all cases. This result indicates that the surface roughness is more dependent on the remelting temperature than on the initial thickness; thus, the remelting temperature should be maintained as high as 150 °C in order to obtain a smooth surface.

Figs. 5c and **5d** compare surface profiles of the 3d-printed specimens before and after remelting, respectively; these photographs were taken from the top view of each specimen. It can be seen that the stepwise profile of the specimen boundary (**Fig. 5c**) was changed smoothly as shown in **Fig. 5d**.

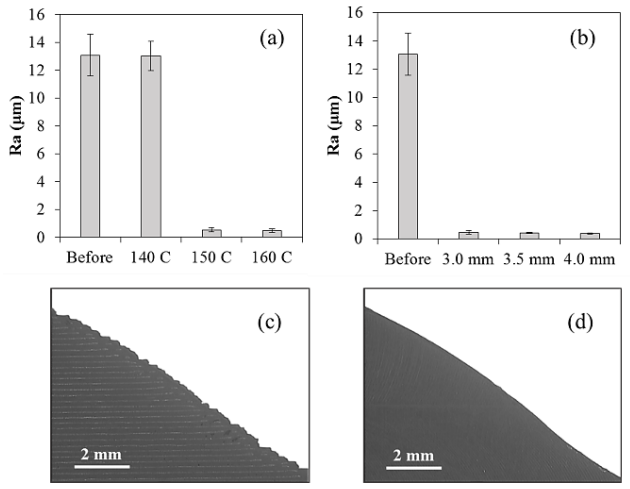

Fig. 5. (a) Surface roughness according to remelting temperature (initial thickness: 3.0 mm), (b) Surface roughness according to initial thickness (remelting temperature: 160ºC), (c) Surface profile before remelting, (d) Surface profile after remelting (160°C remelting temperature and 4.0 mm thickness).

Mechanical strength

Fig. 6a compares the variation in tensile strength according to the remelting temperature for the specimens with 3.0 mm initial thickness. It can be seen that the tensile strength increased slightly to 17.4 MPa when the remelting temperature was 140 °C; the tensile strength of the pure printed sample was 14.7 MPa, as listed in **Table 1**. The tensile strength then increased significantly in the cases of 150 and 160°C remelting temperatures; the tensile strength was 30.1 MPa for the 150°C remelting case, and 32.7 MPa for the 160°C remelting case. Thus, the remelting temperature should be maintained as high as 160 °C in order to ensure comparable tensile strength to the specimens printed along the *X*- or *Y*-directions (see **Table 1**).

Fig. 6b compares the variation in tensile strength according to the initial thickness for the specimens remelted under the 160°C temperature condition. It can be seen that the tensile strength was slightly higher in the 3.5 mm thick specimen (32.9 MPa) than the 3.5 mm thick specimen (32.7 MPa). On the other hand, the 4.0 mm thick sample had much improved strength, 37.7 MPa. This result indicates that the remelted specimen with 4.0 mm initial thickness ensures tensile strength even higher than the *X*- or *Y*-directionally printed ones.

Figs. 6c and **6d** compare sectional images of the pure printed specimen and the remelted one at a 160°C remelting temperature and 4.0 mm thickness, respectively. While a number of filaments and the corresponding air gaps are observed in the cross-section of the pure printed sample (**Fig. 6c**), there is no air gap nor filament boundary in the remelted sample (**Fig. 6d**). Based on these results, we can conclude that the remelting of the 3d-printed parts requires a high remelting temperature near the melting point of the polymer material and enough additional volume to fill air gaps among a number of laminated filaments.

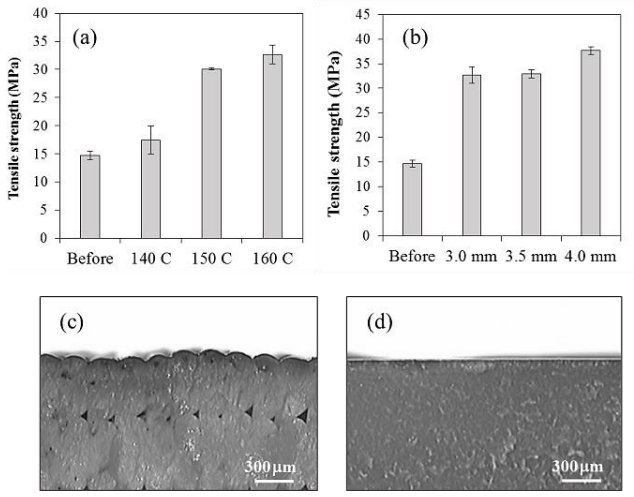

Fig. 6. (a) Tensile strength according to remelting temperature, (b) Tensile strength according to initial thickness, (c) Sectional photograph before remelting, (d) Sectional photograph after remelting (160 °C remelting temperature and 4.0 mm thickness).

Conclusion

This paper presents a new post-processing method for 3d-printed thermoplastic parts. This process, called *constrained remelting*, improves the surface roughness and mechanical strength of the 3d-printed parts which were made by a FDM type printing process. For this purpose, a 3d-printed PLA sample was inserted in a profiled mould insert with a negative shape and was then heated to near the melting temperature with additional thickness. Remelting conditions, the remelting temperature and initial thickness, were investigated in terms of the surface roughness and tensile strength. The results showed that 160°C remelting temperature and 4.0 mm thickness conditions provided the best result in which the *Z*-directionally printed specimens had even higher strength than the *X*- or *Y*-directionally printed ones.

Considering that the proposed remelting process was performed using a desktop type mini-press, this process can be more efficient in manufacturing a small number of

products than the conventional injection mounding process. That is, this process can be used to upgrade a 3d-printed part into an end product by improving its surface roughness and mechanical strength. Although this study used a relatively simple shape (tensile specimen), the proposed process can also be extended to finish complicated parts if the profiled insert is fabricated by metal 3d printing.

Acknowledgements

This study was supported by the Research Program funded by the Seoul National University of Science and Technology.

Author's contributions

Conceived the plan: KP; Performed the expeirments: HCK, DYK; Data analysis: HCK, JEL; Numerical simulation: DYK; Wrote the paper: KP, JEL. Authors have no competing financial interests.

Supporting information

Supporting informations are available from VBRI Press.

References

1. Gibson, I.; Rosen, D. W.; Stucker, B., Additive manufacturing technologies. Springer: New York, **2010**.
DOI: 10.1007/978-1-4939-2113-3
2. Onuh, S. O.; Yusuf, Y. Y., *J. Intell. Manuf.*, **1999,** *10*, *3*, 301.
DOI: 10.1023/A:1008956126775
3. Campbell, I.; Bourell, D.; Gibson, I., *Rapid Prototyp. J.*, **2012,** *18*, 255.
DOI: 10.1108/13552541211231563
4. Mohan Pandey, P.; Venkata Reddy, N.; Dhande, S. G., *Rapid Protoyp. J.*, **2003,** *9*, 274.
DOI: 10.1108/13552540310502185
5. Jones, R.; Haufe, P.; Sells, E.; Iravani, P.; Olliver, V.; Palmer, C.; Bowyer, A., *Robotica*, **2011,** *29*, 177.
DOI: 10.1017/S026357471000069X
6. Turner, B. N.; Gold, S. A., *Rapid Prototyp. J.*, **2015,** *21*, 250.
DOI: 10.1108/RPJ-02-2013-0017
7. Thrimurthulu, K.; Pandey, P. M.; Reddy, N. V., *Int. J. Mach. Tools Manuf.*, **2004,** *44*, 585.
DOI: 10.1016/j.ijmachtools.2003.12.004
8. Byun, H. S.; Lee, K. H., *Int. J. Adv. Manuf. Technol.*, **2006,** *28*, 307.
DOI: 10.1007/s00170-004-2355-5
9. Rahmati, S.; Vahabli, E., *Int. J. Adv. Manuf. Technol.*, **2015,** *79*, 823.
DOI: 10.1007/s00170-015-6879-7
10. Kulkarni, P.; Dutta, D., *J. Manuf. Sci. Eng.*, **1999,** *122*, 100.
DOI: 10.1115/1.538891
11. Pandey, P. M.; Reddy, N. V.; Dhande, S. G., *J. Mater. Process. Technol.*, **2003,** *132*, 323.
DOI: 10.1016/S0924-0136(02)00953-6.
12. Karunakaran, K.; Suryakumar, S.; Pushpa, V.; Akula, S., *Rob. Comput. Integr. Manuf.*, **2010,** *26*, 490.
DOI: 10.1016/j.rcim.2010.03.008
13. Williams, R. E.; Melton, V. L., *Rapid Prototyp. J.*, **1998,** *4*, 56.
DOI: 10.1108/13552549810207279
14. Galantucci, L.; Lavecchia, F.; Percoco, G., *CIRP Ann. Manuf. Technol.*, **2009,** *58*, 189.
DOI: 10.1016/j.cirp.2009.03.071
15. Galantucci, L.; Lavecchia, F.; Percoco, G., *CIRP Ann. Manuf. Technol.*, **2010,** *59*, 247.
DOI: 10.1016/j.cirp.2010.03.074
16. Kuo, C.-C.; Wang, C.-W.; Lee, Y.-F.; Liu, Y.-L.; Qiu, Q.-Y., *Int. J. Adv. Manuf. Technol.*, **2016**, 1.
DOI: 10.1007/s00170-016-9129-8
17. Sood, A. K.; Ohdar, R.; Mahapatra, S., *Mater. Des.*, **2010,** *31*, 287.
DOI: 10.1016/j.matdes.2009.06.016

Supporting information

Numerical simulation for remelting

Numerical simulation was performed to determine the appropriate heating and cooling time for the constrained remelting. ANSYS Multiphysics was used to perform transient thermal finite element (FE) analysis for the given problem. The therrmal properties of the materials are given in **Table 2**.

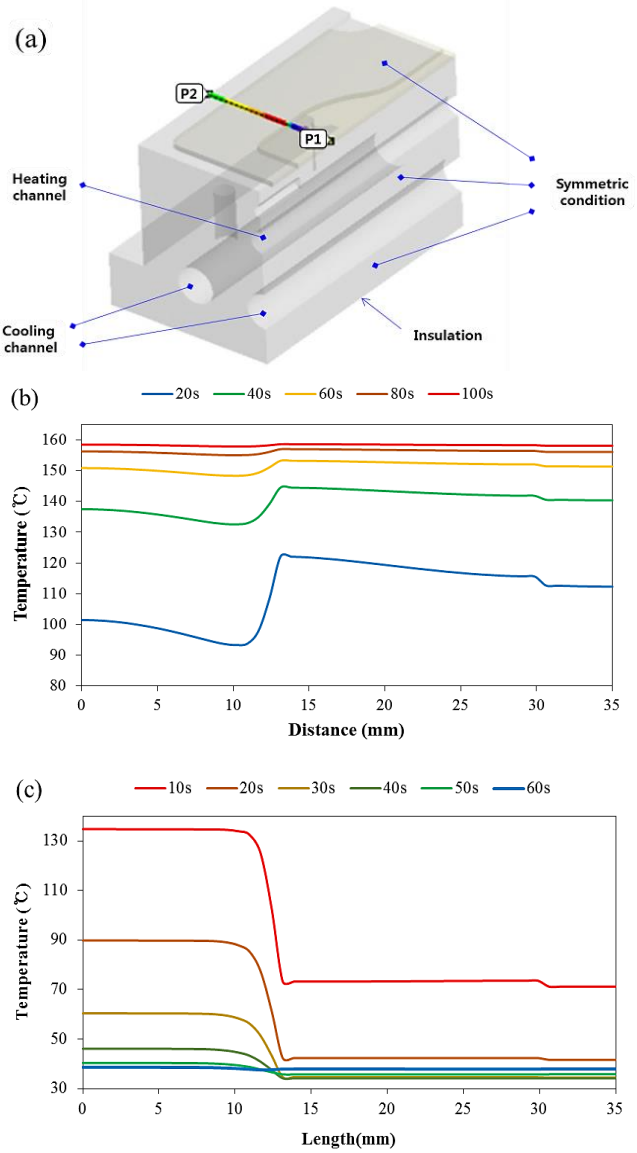

Fig. 7. (a) Analysis domain and boundary conditions for thermal FE analysis, (b) change in temperature profiles during the heating stage, (c) change in temperature profiles during the cooling stage.

Fig. 7a shows the analysis domain and the relevant boundary conditions for the FE analysis. A half model was constructed by considering the symmetric geometry. Themal boundary conditions (heating and cooling conditions) were the same as those of the remelting experiments. Temperature profiles along the path (from P1 to P2 shown in **Fig. 7a**) were compared at vaious time steps both in the heating and cooling stages.

Fig. 7b plots the temperature profiles along the path during the heating stage. It can be seen that the surface temperature underwent a remarkable change at the biginning of the heating stage; at 20 s heating, the temperature in the polymer region (between 0 and 12 mm distance) was lower than 100°C while the temperature in the profiled mould insert (betweem 13 and 30 mm distance) was higher than 115°C. This temperature difference between the polymer and metal regions decreased as the heating time increased, and became negiligible after 100 s heating. Based on this result, the heating time was set to 10 minutes to ensure enough heating for the 3d-printed polmer specimen to be melted and restructured.

Table 2 Thermal properties for the remelting sections.

Material	PLA	AA-6061
Thermal conductivity (W/m-K)	0.13	180
Specific heat (J/kg-K)	1200	896
Density (kg/m^3)	1240	2700

Fig. 7c plots the temperature profiles along the path during the cooling stage, which shows the opposite trend from that of the heating stage. That is, the surface temperature of the polymer region was much higher than that of the metal region due to their difference in thermal conductivity; the resulting temperatire difference was as high as 60°C after 10 s cooling. This temperature difference decreased as the cooling time increased, and became negiligible after 50 s of cooling. Based on this result, the cooling time was set to 1 minute when the whole region was cooled to as low as 35°C.